THE ASTROPHYSICAL JOURNAL, 469:L9–L12, 1996 September 20

MILLISECOND X-RAY VARIABILITY FROM AN ACCRETING NEUTRON STAR SYSTEM

TOD E. STROHMAYER,[1] WILLIAM ZHANG,[1] JEAN H. SWANK,[2] ALAN SMALE,[1] LEV TITARCHUK,[3] AND CHARLES DAY[1]
Laboratory for High Energy Astrophysics, Goddard Space Flight Center, Greenbelt, MD 20771

AND

UMIN LEE
Astronomical Institute, Tohoku University, Sendai, Japan
Received 1996 May 29; accepted 1996 July 10

ABSTRACT

We report the detection with the Proportional Counter Array (PCA) on board the *Rossi X-Ray Timing Explorer* (*RXTE*) of millisecond variability in the X-ray emission from the low-mass X-ray binary 4U 1728−34. Pulsations at 363 Hz with amplitudes (rms) of 2.5%–10% are present in six of the eight bursts analyzed to date. The strongest were seen in two successive bursts recorded on 1996 February 16 when the quiescent count rate was near the highest seen by PCA. The pulsations during these bursts show frequency changes of 1.5 Hz during the first few seconds but become effectively coherent as the burst decays. We interpret the 363 Hz pulsations as rotationally induced modulations of inhomogeneous burst emission. This represents the first compelling evidence for a millisecond spin period in a low-mass X-ray binary. Complex, intensity-dependent, millisecond X-ray variability is also present in all the quiescent flux intervals we examined. Most interesting was the behavior as the count rate approached its highest observed level. Two quasi-periodic oscillations (QPOs) were simultaneously observed in the 650–1100 Hz range. Both QPOs increased in frequency together, maintaining a nearly constant frequency separation of about 363 Hz, the spin period inferred from the burst oscillations. This phenomenology is strongly suggestive of the magnetospheric beat frequency model proposed for the horizontal-branch oscillations (HBOs) seen in Z sources. We discuss this and several other possible physical interpretations for the observed X-ray variability.

Subject headings: stars: neutron — stars: rotation — X-rays: stars

1. INTRODUCTION

A variety of physical processes acting on or in the vicinity of a neutron star have characteristic timescales in the millisecond regime. For example, the oscillation spectrum of neutron stars ranges from <0.1 to several tens of milliseconds (see McDermott, Van Horn, & Hansen 1988 and references therein) and Keplerian orbits within one stellar radius have millisecond periods. Further, recent work by Klein et al. (1996) suggests that magnetically dominated accretion onto neutron stars can produce photon bubble oscillations (PBOs) with periods in the millisecond regime. Two classes of Galactic, accreting low-mass X-ray binaries (LMXB), the so-called Z and atoll sources, have now been postulated based on their correlated X-ray timing and spectral behavior (Hasinger & van der Klis 1989, hereafter HVK). 4U 1728−34 is a well-known, X-ray bursting LMXB (Lewin 1976; Basinska et al. 1984), which has been classified as an atoll source based on observations with the *EXOSAT* satellite (HVK). Its orbital period is unknown, and an optical counterpart has yet to be identified. Previous observations with *EXOSAT* of the X-ray variability of 4U 1728−34 in the low-intensity (low-$\dot{M}$) "island" state showed a flat excess of non-Poissonian power above 0.1 Hz with an exponential cutoff around 30 Hz and no evidence of QPOs at frequencies up to 100 Hz (HVK). There have been reports of QPO-like peaks in the 1–60 Hz power spectra of some atoll sources (Yoshida et al. 1993; Lewin et al. 1987; Dotani et al. 1989). A previous report of a 12 ms periodicity during a burst (Sadeh et al. 1982) is to our knowledge the only previous report of high-frequency periodic behavior in this source.

In this Letter we report new observations with the Proportional Counter Array (PCA) on board NASA's *Rossi X-Ray Timing Explorer* (*RXTE*) of the X-ray variability of this source at frequencies up to 4 kHz. These observations reveal a wealth of new high-frequency X-ray variability in both the bursting and persistent emission that is likely due to processes occurring on or in the near vicinity of the neutron star in this system. Preliminary reports of this work have been made in Strohmayer, Zhang, & Swank (1996a) and Strohmayer et al. (1996b). We begin in § 1 with a brief summary of the observation campaign carried out and the data obtained. We describe the burst oscillations in § 2. In § 3 we summarize the variability observed in the persistent emission. In § 4 we discuss some possible physical interpretations for the observed variability.

2. OBSERVATIONS AND DATA DESCRIPTION

We observed 4U 1728−34 on eight occasions over the period 1996 February 16.0 UT to February 29.96 1996 UT, obtaining 55 hr of good observing time. Over the course of these observations, the total quiescent count rate in PCA varied from a low of 1100 counts s^{-1} to a high of 2300 counts s^{-1}. Of this, typically 100 counts s^{-1} were background in the PCA. The source was burst active during the entire campaign, and a total of 11 type I X-ray bursts were observed.

The PCA experiment on *RXTE* is an array of five identical multiwire proportional counters with an area of ≈6250 cm^2

[1] Also USRA/LHEA, Mail Code 662, NASA/GSFC Greenbelt, MD 20771.
[2] LHEA, Mail Code 662, NASA/GSFC Greenbelt, MD 20771.
[3] Also George Mason University.

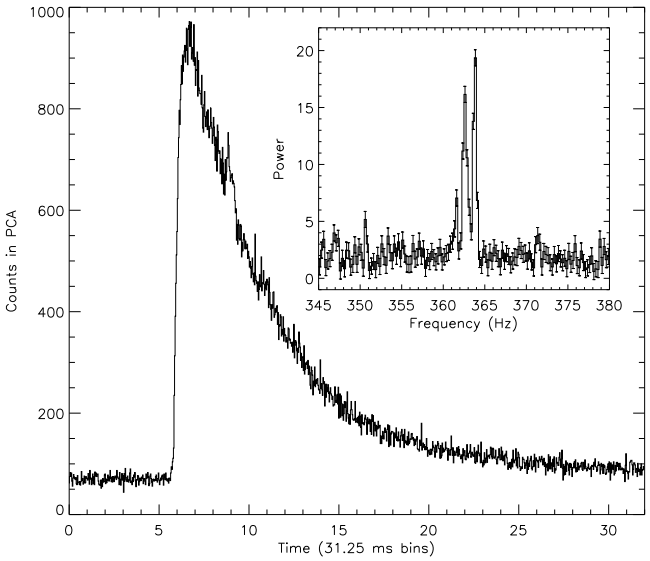

FIG. 1.—Light curve of the burst that occurred at 10:00:45 UTC on 1996 February 16. The main panel shows the total PCA counts in 31.25 ms bins. The inset panel shows a portion of the power spectrum computed from 32 s of 122 μs data. Each bin is 0.25 Hz wide and represents the average of eight original power spectral bins. The error bars include only the uncertainties due to Poisson counting statistics.

(Zhang et al. 1993) and is capable of time-tagging individual X-ray events to 1 μs resolution. To obtain high time resolution monitoring of the quiescent flux we employed a 122 μs (1/8192 s) single-bit data mode with no spectral information for the bulk of the observing time. After initial study of the single-bit mode data indicated the presence of kilohertz variability, we additionally acquired X-ray event data with 16 μs resolution and 64 energy channels over the 2–60 keV range. A set of burst trigger and catcher modes were always present to record burst data at high time and spectral resolution. A set of standard modes provided 1/8 s timing data and 16 s spectral measurements in 129 energy channels for the entire observing campaign.

3. X-RAY VARIABILITY OF BURSTS

To date we have been able to analyze eight of the 11 bursts observed, but here we will discuss results from only one of the bursts in detail. Figure 1 shows the time history of the burst that triggered the EDS on 1996 February 16 at 10:00:45 UTC. Just prior to this burst, the quiescent count rate in PCA was 2250 counts s^{-1}, near the highest observed. We calculated an FFT power spectrum using 32 s of 122 μs time-resolution data starting just prior to the burst onset. The resulting power spectrum, rebinned by a factor of 8, is shown in the inset panel of Figure 1. The complex oscillatory behavior at 363 Hz is clearly evident. We next computed a dynamic power spectrum across the burst profile using 1 s intervals of the same data. A false-color image was produced by stacking the individual spectra and is shown in Figure 2 (Plate L2). The dynamic spectrum reveals that the individual peaks in Figure 1 are due to evolution of the pulsations through the burst. The pulsations are easily detected in the initial rise of the burst, with an amplitude (rms) of about 10%, the highest measured. The amplitude drops below the 1 s detection level of about 1.5% near burst peak and then increases again, varying up and down between 3% and 7% through the duration of the burst. In addition, the centroid frequency of the oscillation increased from about 362.5 to 363.9 Hz as the burst progressed, becoming effectively coherent in the burst tail. Another burst recorded about 3 hr earlier showed very similar pulsation properties. A total of six of the eight bursts so far analyzed show significant oscillations centered near 363 Hz, but only the two observed on 1996 February 16 show the complex time evolution illustrated in Figure 2.

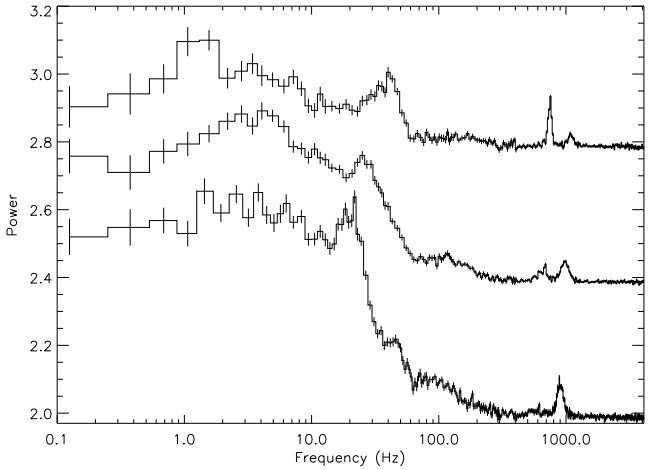

FIG. 3.—Average power spectra computed from 1996 February 15 at 11:50:22 to February 16 at 10:13:01 UTC showing the evolution of the two kilohertz QPOs. The source count rate was increasing from figure bottom to top. Also note the QPO between 20 and 40 Hz and the broadband noise component between 0.1 and 10 Hz that decreases in strength as the source intensity increases. The Nyquist frequency is 4096 Hz in each panel, and the small dead-time correction to the Poisson level has not been subtracted. For clarity, the two upper curves have been displaced by 0.4 and 0.8, respectively

4. PERSISTENT FLUX X-RAY VARIABILITY

We summarize here only the most interesting features of the variability seen as the source count rate increased to the maximum observed. A more complete description of the quiescent X-ray variability will appear elsewhere. This interval spans 1996 February 15 at 11:50:22 UTC to February 16 at 10:13:01 UTC. Over this period, the total count rate in PCA climbed rather steadily from 1900 counts s^{-1} to near 2300 counts s^{-1}. For all data in this interval, we computed FFT power spectra to 4 kHz for 8 s subintervals using the 122 μs time series data. We averaged the individual 8 s power spectra to obtain reasonable statistics through the interval. Figure 3 shows three snapshots of the power spectral evolution through this interval. The count rate and time both increase from figure bottom to top. Each curve represents the average of 2–3 hr of data. The power normalization is such that the Poisson fluctuations around a constant count rate produce a flat spectrum with $P = 2$. The dead-time effects in PCA at these modest count rates are on the order of 1%–2% and serve only to shift down the Poisson level by a constant amount between 0.008 and 0.015 over the range of count rates observed from 4U 1728−34 (Zhang et al. 1995) and have not been subtracted in the figure shown.

The power spectra are complex, revealing two QPO features in the 600–1100 Hz range, a relatively flat noise excess between 0.1 and 20 Hz, QPOs between 20 and 40 Hz, and a broad weak excess of power in the 70–200 Hz range. In the lower curve, the QPOs at 900 Hz can be fitted with a Lorentzian profile with a width (FWHM) of 64 $\pm$ 3.5 Hz and

TABLE 1

KILOHERTZ QPO EVOLUTION IN 4U 1728−34

T_{start} (UT)	T_{end} (UT)	C (counts s^{-1})	ν_1 (Hz)	ν_2 (Hz)	$\delta\nu$ (Hz)	A_1 (percent)	A_2 (percent)
01:49:20.....	03:57:05	2076.5 ± 0.6	637.5 ± 3.6	988 ± 5.9	351.1 ± 7	5.2	8.1
03:58:21.....	04:29:58	2106.2 ± 1.0	682.6 ± 2.2	1045.4 ± 6.2	362.8 ± 6	6.0	7.1
06:24:14.....	06:41:17	2136.5 ± 1.4	716.0 ± 1.1	1058.3 ± 12.1	342.3 ± 12	6.9	5.5

an rms amplitude of about 8%. As time goes on and the source intensity increases, the higher frequency kilohertz QPO feature weakens as a lower frequency QPO appears and increases in both frequency and amplitude. The lower frequency feature narrows as the count rate increases, eventually reaching a width (FWHM) of about 6.5 Hz, corresponding to a Q value of about 120 at an amplitude of 6.3%. We have investigated the temporal evolution of the kilohertz QPOs in Figure 3. Table 1 summarizes the results of fits to both QPO features over three consecutive time intervals when both features were present. We give the average source count rate, best-fit centroid frequency, frequency separation between the two features, and amplitude (rms) of each feature. In Table 1, the subscripts 1 and 2 denote the lower and higher frequency QPOs, respectively. The QPO features track each other over more than 100 Hz in frequency space. During this evolution, the separation of the QPO centroids remains nearly constant at about 360 Hz with a 1 σ uncertainty on the frequency difference ranging from about 6 to 12 Hz depending on the interval examined. This separation is very close to the frequency of the oscillations observed during the bursts. This phenomenology is suggestive of the beat frequency model for QPOs proposed to explain the horizontal-branch oscillations (HBOs) observed in Z sources (Alpar & Shaham 1985; Lamb et al. 1985); however, in this case, if true, we are observing directly for the first time all three frequencies responsible for the phenomenon. We will comment on this possibility at more length in the discussion section.

We have been able to track the centroid frequency of the highest frequency QPOs over a wider range of source intensities than the lower frequency QPOs. We show in Figure 4 a plot of the intensity versus centroid frequency for both QPO features. The positive correlation between frequency and intensity is striking. The best-fit power law for the highest frequency QPO has an index of $\alpha = 1$; although the functional form given in the figure describes the frequency-intensity trend qualitatively, we emphasize that it does not provide a good statistical description of the data.

Using the 16 μs, 64 energy channel event data, we investigated the behavior of the narrow 800 Hz QPO feature as a function of photon energy. The amplitude (rms) of this feature is a strong function of energy, ranging from about 3% in the 2–6 keV band to 9.5% for photons above 12 keV. We used the 16 s, 129 channel spectral accumulations to construct an X-ray color-color diagram for sections of the data. Using three spectral bands, $c_1 = 3$–6 keV, $c_2 = 6$–9 keV, and $c_3 = 9$–12 keV, and 64 s accumulations per point, we find a positive correlation of the intensity with softness. The appearance of the strongest red noise excess in the 0.1–10 Hz regime in the lowest intensity states observed by *RXTE*/PCA is consistent with the argument that the low count rate state corresponds to an island state in this source (see van der Klis 1995).

5. DISCUSSION

We believe that stellar rotation is the simplest and most plausible explanation for the 363 Hz oscillations observed during the bursts. The inferred spin period is consistent with theoretically expected periods in LMXB (Smarr & Blandford 1976; Verbunt & van den Heuvel 1995) as well as the observed periods of ostensibly recycled millisecond radio pulsars and provides long-sought direct evidence linking the LMXBs and millisecond radio pulsars. Rotational modulation of thermonuclear flash inhomogeneities can plausibly explain the 5%–10% amplitudes observed (Bildsten 1995). Further, the evolution to an essentially coherent signal in the burst tail is suggestive of a highly coherent mechanism such as rotation. We suggest that the frequency variability observed during the burst rise and near peak emission can be explained in terms of motion of the thermonuclear burning front on the stellar surface. This frequency change can be as large as $\delta\nu \approx \nu_{burn} \approx 1/\tau_{rise}$, where τ_{rise} is the burst rise time, i.e., the time it takes the burning front to travel around the star. The observed subsecond rise times (≈0.5 s) imply a frequency change in the range of a few Hz, consistent with that observed. We note that Schoelkopf & Kelley (1991) have previously suggested the same mechanism to explain oscillations observed in a burst from Aql X-1.

The crust of a neutron star can support oscillation modes with periods in the 0.7–1 kHz range (McDermott et al. 1988; Strohmayer et al. 1991); however, the complex frequency

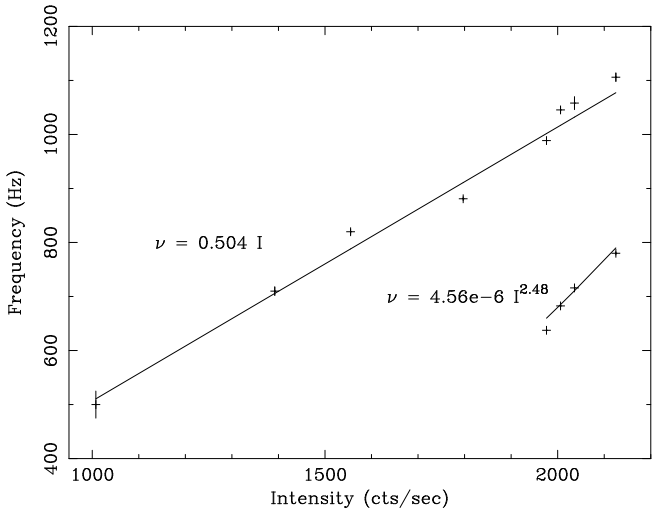

FIG. 4.—Frequency vs. source intensity relation for both kilohertz QPO features. The drawn functional forms are the best-fit power laws to each data set, but they are meant only to characterize qualitatively the correlations and do not adequately describe the data in a statistical sense. A simple estimate of the background count rate has been subtracted from the total observed to obtain each source intensity measurement.

evolution with source intensity and therefore mass accretion rate as well as the large observed oscillation amplitudes argue against stellar oscillations as the cause of the quiescent variability. The observed behavior of two kilohertz QPO peaks both increasing in frequency together while maintaining a nearly constant centroid separation is strongly suggestive of the beat frequency model. The fact that the observed frequency separation is consistent with the spin frequency implied from the burst oscillations is further evidence for this model. In this interpretation, the highest frequency QPO would be due to the orbital modulation of density inhomogeneities in the inner accretion disk. The decay of this signal at the highest source intensities (mass accretion rates) is consistent with the properties expected assuming the model is valid for the HBO observed in Z sources (see Lamb et al. 1985 and van der Klis et al. 1996). The second, lower frequency QPO is then the beat frequency between the orbital and spin frequencies of the neutron star, and the spin period is only directly manifested during bursts. The energy dependence of the amplitude of the putative beat frequency QPO in this interpretation is also similar to that observed in the HBO (Vaughan et al. 1994).

If orbital motion around the neutron star produces variability, then the radius required to obtain period P is $r_{\rm Kep} \approx (GMP^2/4\pi^2)^{1/3} \approx 19$ km for a $M = 1.4$ solar mass neutron star and a period of 800 Hz. The distance to 4U 1728−34 is not well constrained, but assuming that the flux is near-Eddington during the peaks of X-ray bursts, we can scale the observed peak burst count rate observed in PCA to the quiescent count rate to obtain a rough estimate of the accretion rate. This yields an estimate of $\dot{m} \approx 0.06\, \dot{m}_{\rm Edd}$ at the highest quiescent intensities. The lack of coherent pulsations as well as the presence of type I X-ray bursts argues that the magnetic field is likely within the range $B_s = 10^8$–10^9 G. Corresponding values of r_m/R_{ns} for this accretion rate and with B between 10^8 and 10^9 G range from ≈0.5 to 5, which does indeed bracket the value derived assuming the variability is related to a Keplerian frequency.

Klein et al. (1996) have recently investigated the structure of the accretion column in strong field pulsars. They confirm the prediction of Arons (1992) that a "photon bubble" instability occurs within the accretion column. In their calculations, these photon bubbles create millisecond-scale X-ray variability in the frequency range observed in 4U 1728−34, Sco X-1, 4U 1608−52, and recently 4U 1636−54 (see Zhang et al. 1996). Their calculations predict that the photon bubble oscillation (PBO) frequencies should decrease as source intensity increases, contrary to what is observed from 4U 1728−34 and Sco X-1. However, their calculations were performed for high magnetic field conditions, whereas the Z and atoll sources are likely low field objects. More extensive PBO calculations at weaker fields will be required to adequately confront this model.

Finally, Titarchuk & Lapidus (1996) suggest that acoustic oscillations in the postshock boundary layer surrounding the neutron star may be the cause of the observed variability. In this model, the boundary region must have a size $l \approx 8 \times 10^5\, T_5^{1/2}/\nu_1$ cm, where $T_5 = T_e/5$ keV and $\nu_1 = \nu/1$ kHz, with T_e and ν_1 the electron temperature and oscillation frequency respectively, which is reasonably consistent with hydrodynamical calculations of the shock region (Chakrabarti & Titarchuk 1995). Detailed comparison of the QPO frequency and spectral evolution should allow a serious test of this model.

T. S. acknowledges the support of the visiting scientists program under the Universities Space Research Association (USRA contract NAS5-32484) in the Laboratory for High Energy Astrophysics (LHEA) at Goddard Space Flight Center.

REFERENCES

Alpar, M. A., & Shaham, J. 1985, Nature, 316, 239
Arons, J. 1992, ApJ, 388, 561
Basinska, E. M., Lewin, W. H. G., Sztajno, M., Cominsky, L., & Marshall, F. J. 1984, ApJ, 281, 337
Bildsten, L. 1995, ApJ, 438, 852
Chakrabarti, S., & Titarchuk, L. 1995, ApJ, 455, 623
Dotani, T., Mitsuda, K., Makishima, K., & Jones, M. H. 1989, PASJ, 41, 577
Hasinger, G., & van der Klis, M. 1989, A&A, 225, 79 (HVK)
Klein, R. I., Arons, J., Jernigan, J. G., & Hsu, J. J-L. 1996, ApJ, 457, L85
Lamb, F. K., Shibazaki, N., Alpar, M. A., & Shaham, J. 1985, Nature, 317, 681
Lewin, W. H. G. 1976, IAU Circ., 2922
Lewin, W. H. G., et al. 1987, MNRAS, 226, 383
McDermott, P. N., Van Horn, H. M., & Hansen, C. J. 1988, ApJ, 325, 725
Sadeh, D., et al. 1982, ApJ, 257, 214
Schoelkopf, R. J., & Kelley, R. L. 1991, ApJ, 375, 696
Smarr, L. L., & Blandford, R. D. 1976, ApJ, 207, 574
Strohmayer, T. E., Ogata, S., Iyetomi, H., Ichimaru, S., & Van Horn, H. M. 1991, ApJ, 375, 679
Strohmayer, T. E., Zhang, W., & Swank, J. H. 1996a, IAU Circ., 6320
Strohmayer, T. E., et al. 1996b, IAU Circ., 6387
Titarchuk, L., & Lapidus, I. 1996, in preparation
van der Klis, M. 1995, in X-Ray Binaries, ed. W. H. G. Lewin, J. van Paradijs, & E. P. J. van den Heuvel (Cambridge: Cambridge Univ. Press), 252
van der Klis, M., et al. 1996, in preparation
van Paradijs, J., et al. 1996, IAU Circ., 6336
Vaughan, B., van der Klis, M., Lewin, W. H. G., Wijers, R. A. M. J., van Paradijs, J., Dotani, T., & Mitsuda, K. 1994, ApJ, 421, 738
Verbunt, F., & van den Heuvel, E. P. J. 1995, in X-Ray Binaries, ed. W. H. G. Lewin, J. van Paradijs, & E. P. J. van den Heuvel (Cambridge: Cambridge Univ. Press), 457
Yoshida, K., Mitsuda, K., Ebisawa, K., Ueda, Y., Fujimoto, R., & Yaqoob, T. 1993, PASJ, 45 605
Zhang, W., Giles, A. B., Jahoda, K., Soong, Y., Swank, J. H., & Morgan, E. H. 1993, Proc. SPIE, 2006, 324
Zhang, W., Jahoda, K., Swank, J. H., Morgan, E. H., & Giles, A. B. 1995, ApJ, 449, 930
Zhang, W., Lapidus, I., White, N. E., & Titarchuk, L. 1996, ApJ, submitted

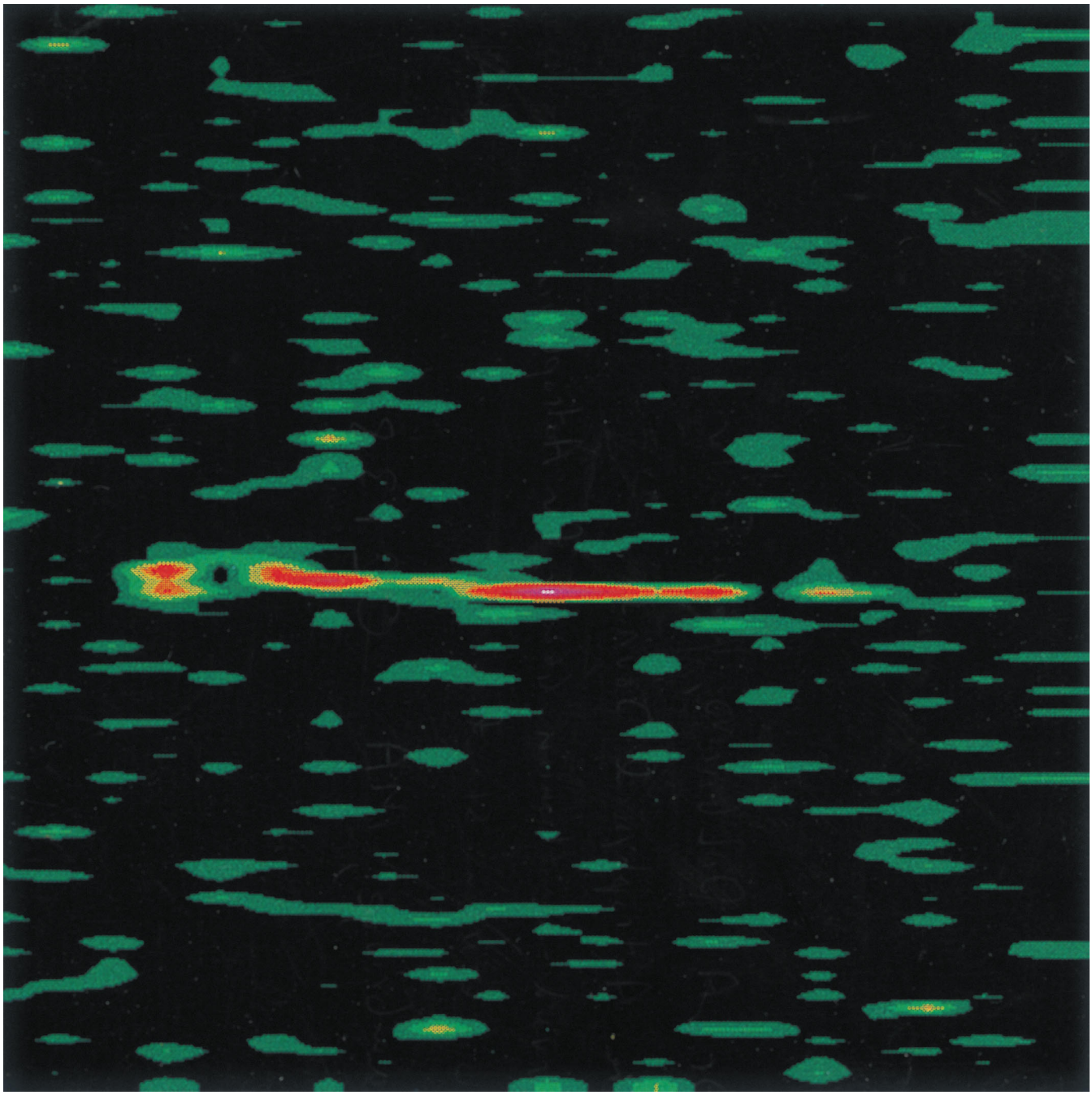

FIG. 2.—Image of the dynamic power spectrum during the burst shown in Fig. 1. The color map shows increasing power in the order green, red, blue, and white. The vertical axis, from figure top to bottom, denotes a linear frequency scale from 313 to 412 Hz, and time increases along the horizontal axis with a resolution of 1 s. The total time shown is 16 s.

STROHMAYER et al. (see 469, L10)